SCTB14 Working Paper

SKJ-2

SEPODYM Skipjack Analysis

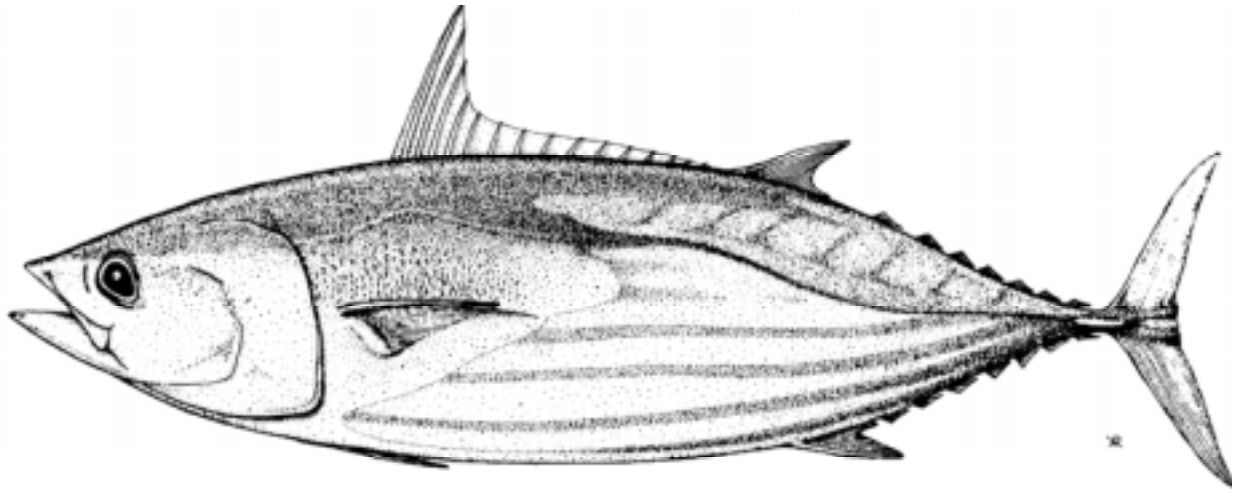

Patrick Lehodey

Oceanic Fisheries Programme
Secretariat of the Pacific Community
Noumea, New Caledonia

SEPODYM Skipjack Analysis

Patrick Lehodey

Background

To explore the underlying mechanisms by which the environmental variability affects the pelagic ecosystem and tuna populations, a spatial environmental population dynamic model (SEPODYM) has been developed at the OFP-SPC (Bertignac *et al.* 1998; Lehodey *et al.* 1998; Lehodey 2001). The model is a 2D coupled physical-biological interaction model at the scale of ocean basin, combining a forage (prey) production model with an age structured population model of targeted (tuna predator) species. The model contains environmental and spatial components used to constrain the movement and the recruitment of tuna. Input data set for the model are sea surface temperature, oceanic currents, and primary production data that can be predicted from coupled physical-biogechemical models, as well as satellite-derived data distributions. Development and test of a first version of the model were carried out in 1995 with climatological series of predicted currents from the OPA ocean model (LODYC) and CZCS-satellite-derived chlorophyll data as a proxy of the primary productivity. Results were in agreement with the general knowledge on the spatial distribution of this species. However, the spatial correlation between predicted and observed catch remained very low and it became clear that the inter-annual variability due to the El Niño Southern Oscillation (ENSO) had to be taken into consideration. Particularly as other results based on fishery and tagging data demonstrated the importance of ENSO on the movement of skipjack (Lehodey *et al.* 1997). Predicted data from a biogeochemical model coupled to an Ocean General Circulation model developed at the LODYC (Stoens *et al.* 1999) allowed testing the impact of interannual variability on the forage in the equatorial 20N-20S area (Lehodey et al., 1998).

In 1999, an important development in the modelling concerned the interaction between predicted tuna density and forage density, that is the coupling between the forage (prey) and tuna (predator) population. The modelling approach was presented during the 13th SCTB (Lehodey 2000) and tested with the previous LODYC's run of new primary production. Despite some limitations in the input data set and a simplified parameterization, this first simulation improved the prediction of catch and was helpful to interpret the observed ENSO-related spatio-temporal changes in the distribution of skipjack population (Lehodey 2001). However, the run included a short time-series (1992-95) and was limited to the 20^{o}N–20^{o}S equatorial region when tuna stocks extend to sub-tropical and temperate oceanic regions. The opportunity to consider a longer time-series over the whole Pacific basin arose with the recent developments in a NPZ (Nutrients-Phyto-Zooplankton) model developed by F. Chai & M. Jiang (University of Maine), R.T. Barber (Duke University), R. Dugdale & F. Wilkerson (San Francisco University), T.H. Peng (AOML/NOAA) and Y. Chao (JPL/NASA).

(SEPODYM web page: http://www.spc.int/OceanFish/Html/TEB/Env/sepodym_intro.htm)

NPZ model

The NPZ model is driven by a physical model that is a full 3D-ocean general circulation model (OGCM). The baseline of the physical model is the Module Ocean Model (MOM) developed at the GFDL/NOAA, Princeton. The model covers the entire Pacific except the Southern Ocean section (Li et al., 2001). The resolution is 2 deg. in longitude, 0.5 deg near the equator (10S to 10N), and 2 deg. close to the north and south boundaries. There are 40 layers with 10m resolution within the euphotic zone (120m). The surface forcing uses COADS monthly averaged fields from 1950 to 1993, with a restoring surface salinity process back to Levitus climatological value. The NPZ model (Chai *et al.* 2001) has 10 components with two nutrients (nitrate and silicate). It simulates the equatorial region very well with elevated high biomass in the cold tongue region, as well as the subarctic area. The modeled simulated spatial pattern agrees well with the SeaWiFs satellite observed data. The model simulates all El Niño events well with higher temperature anomaly during the El Niño, and cooler temperature during the La Niña. The temperature simulation indicates the physical model and surface forcing are reasonably set up although there are still some discrepancy in the high latitude. In the equatorial upwelling region, the total phytoplankton biomass for the top 120m decreases during all five El Niño events, not just near the surface but throughout the water column. The strongest reduction of the phytoplankton biomass occurred during the 1982-83 El Niño, and followed by 1972-73 El Niño. The highest biomass periods are 1987-88 and 1974. Beside the strong interannual variability, nitrate concentration tends to be higher before 1975-76, in comparison with the 1980s. This is related to the Pacific decadal oscillation (PDO).

Currents and primary production are averaged over the euphotic layer and interpolated with the sea surface temperature (SST) on a grid of one-degree square resolution to be used with SEPODYM.

Tuna Forage

Instead of developing a detailed explicit food web through the whole pelagic ecosystem, the tuna forage is considered as a single population (Fig. 1). Since all the organisms of the same cohort have the same age, it is immaterial whether the cohorts are of the same species or not. The classical fish population approach is used to describe the dynamics of this forage population with a continuous recruitment (S) and a mortality coefficient (λ). The development of a new primary biomass during a period of time (P: primary production) allows the development of a new cohort of many different organisms, a fraction of which will be recruited after a time T_r in the forage population. The level of fraction transferred depends of an ecological transfer coefficient (0.04 according to Iverson (1990)). In an equilibrium situation, the biomass $F \sim S/\lambda$ and the production $F' = S$.

λ and T_r which characterize F can be estimated using biological characteristics of key-species representative of the forage population using the notion of “mean age” and “maximum life span” defined as $(T_r + 1/\lambda)$ and $(1/\lambda \,.\, \mathrm{Ln}(0.01) + T_r)$ respectively (see Lehodey 2001). A mean age of 150 days (d) was chosen with a value of 60 d for T_r. This lead to a maximum life span of 474 d. These values appear to be a reasonable characterization of tuna forage according to biological studies of typical prey species.

The movement of forage organisms is described with a diffusion-advection equation, using zonal (u) and meridional (v) components of the current for the advective terms in the two horizontal dimensions and a diffusion coefficient reproducing both diffusion of water and random movement of organisms. Extensive description of the mathematical model used for the transport can be found in Sibert and Fournier (1994), Bills and Sibert (1997) and Sibert *et al.* (1999). The differential equations are numerically solved by finite-difference techniques using a network of regularly spaced grid points and a discrete time step. The upwind differencing scheme (Press *et al.* 1992) is used for approximating the first derivatives in the advection terms.

Tuna habitat

Adult habitat index

The adult habitat index (H_a) simply combines the spatial distribution of forage with a temperature function defined for each tuna species (Fig. 2). This index is used in the model to constrain the movement of young and adult tuna. The tuna movement is described with an advection-diffusion equation as for the forage. However, for tuna the advection term is proportional to the gradient of the habitat with X_o the coefficient of proportionality. At this stage of development, this coefficient is constant whatever the age. However, to consider change in tuna behaviour according to the quality of habitat, e.g., leaving rapidly a poor habitat region, a function is used to increase the diffusion (D) and the advection (X_o) at low values of habitat index (Fig. 3). The parameterization is scaled to be in agreement with the range of values estimated from tagging data by Sibert *et al.* (1999).

Spawning habitat index and recruitment

A spawning habitat index (H_s) is used to constrain the recruitment to environmental conditions. In each point of the grid, the number of recruit is given by a recruitment value proportional to the spawning habitat index. The recruitment value is used to scale the total biomass to independent estimates. The basic assumption to define this index is that the spawning area is limited by the presence of mature tuna and by sea surface temperature (SST) above a limit value. This latter condition is supported by the high correlation found between SST and occurrence of reproductively-active tropical tuna (Schaefer 1998). The spawning temperature function (θ_s) used is shown in Figure 4.

However, other environmental effects are investigated. With temperature and physical constraints like the advection creating favourable zones of retention for larvae, and that are already considered in the model, the food availability and the predation are likely the other major factors that affect larval survival and pelagic fish recruitment. Food of larvae is directly dependent on primary production, while their predators are organisms included in the tuna forage. Therefore, it was interesting to investigate these two opposite effects on the recruitment by using the ratio P/F. The following equation is used to calculate H_s:

$$H_s = \theta_s \, e^{(\alpha \, \mathrm{Ln}(P/F))}$$

and four values were tested for α : $\alpha = 0$ ($H_s = \theta_s$), $\alpha = 0.5$, $\alpha = 0.75$ and $\alpha = 1$ ($H_s = \theta_s \, P / F$).

As the value of α increases, areas characterized by high primary production and low forage (high P/F ratio) have higher positive impacts on recruitment (Fig. 4).

Tuna population

The tuna population and fisheries dynamics simulation sub-model in SEPODYM is a spatial multigear, multispecies model. It is age-structured to account for growth and gear selectivity on a quarterly basis. It includes a movement model based on a diffusion-advection equation and the gradient of a habitat index (cf. above). A description of the population dynamics can be found in Bertignac et al. (1998). Growth and mortality-at-age estimates from MULTIFAN-CL are used in SEPODYM (Fig. 5). However a function allows an increase in the mortality at very low values of habitat index to prevent the presence of tuna (artificially due to the diffusion equation) in very unfavourable areas (Fig. 5).

The total level of recruitment (or spawning) is adjusted, so that the stock biomass estimates are roughly equal to those obtained independently with MULTIFAN-CL estimates. While MULTIFAN-CL produces recruitment and biomass estimates from robust statistical methods, SEPODYM recruitment and biomass are predicted only from environmental constraints. Therefore, comparisons of fluctuations in time and by region between these two independent estimates are useful to investigate hypotheses on the mechanisms of recruitment.

Tuna Fisheries

Three different fishing gears are described: purse-seine, pole-and-line and a group of mixed domestic gears from the Philippines and Indonesia. A total of ten fleets are represented (Table 1), each with separate catchability coefficients. An age-based selectivity function is used for each gear (Fig. 6). Fishing effort of each fleet varies by month and in space, with a one degree square resolution except for the Philippine and Indonesia fleets that provide data aggregated by five degree square, and year. The catchability coefficients are scaled to obtain estimated catches at the same level as observed catches. Results of the simulation are compared to observed fishing data by fleets, such as total monthly catch, spatial distribution of catch, and distribution of length frequencies.

Limitation

The physical simulation showed a discrepancy in temperature, the current physical model tending to be colder at high latitudes. This is illustrated on Figure 7 where average SST in the area 35N-40N, 140E-180E is compared between the physical model used for the NPZ and SEPODYM simulation and the model used by the National Climate and Environmental Programme (NCEP, USA) that assimilates observed temperature data. Several reasons may contribute to this discrepancy (F. Chai, pers. comm.): (i), the resolution is not high enough in the region near Japan (2 degree in longitude x 1 degree in latitude), so the northward heat transport by Kuroshio Current is insuficient; (ii) there is no sea ice dynamics, so the sea temperature can be lower than –4 degree during the winter, the NCEP and any other observed SST will set it to zero; (iii) the heat flux from COADS may not be right.

This discrepancy has important consequences on the prediction of the catch by the seasonal summer fishery off Japan. Therefore, predicted catch in this region will be not considered in the analysis of the present SEPODYM simulations.

Results

Results of the simulations can be separated into two groups. The first one concerns the simulation with recruitment only dependent on SST ($\alpha = 0$) and the second, simulations with the additional effect related to the P/F ratio ($\alpha > 0$). The total recruitment and biomass estimates for the six regions used in MULTIFAN-CL skipjack application (Fig. 8) are extracted from the SEPODYM prediction to be compared with the MULTIFAN-CL estimates. A summary of simulations for the four different values of α is given in Table 2. With the exception of the Japanese pole and line fleet and for the reasons related to the limitations on these simulations, the correlation between predicted and observed total monthly catch by fleet is high in all cases with a tendency to a slight decrease as the value of α increases. An illustration is given in Figure 9. The same tendency is observed (Table 2) for the spatial correlation between predicted and observed catch at the resolution of one month and one degree square (Figure 10).

However, the tendency is reversed when comparisons with MULTIFAN-CL estimates of recruitment and biomass are concerned (Table 2, Fig. 11 and 12). When the spawning habitat index is only dependent on SST ($\alpha = 0$) the recruitment and biomass do not show any large fluctuation as suggested by the MULTIFAN-CL analysis. Using P/F ratio ($\alpha > 0$) in the spawning habitat index produces fluctuations showing an evident correlation with the MULTIFAN-CL estimates. For the three values of $\alpha > 0$, the general pattern of the temporal fluctuations remains the same but the amplitude (and the correlation) increases with the increasing value of α. Similar amplitudes to those obtained with MULTIFAN-CL occur for values of α above 0.75. When areas are considered individually (Table 2, Fig. 13), the correlation is the highest in regions 5 and 6 where the largest proportion of the population occurs. In the regions 2 and 3, there is a large discrepancy in the level of recruitment that is likely due to the bias in the temperature preventing high density of skipjack to move in these areas.

The high spatial correlation between observed and predicted catch even with a relatively homogeneous recruitment depending of SST only ($\alpha = 0$) suggests that the dynamics are relatively well described in the model, at least at this large spatial scale. In particular, the redistribution of larvae by currents and the movement of young and adults tuna constrained by the habitat index are fundamental processes to explain the distribution of the population.

The opposite tendency that is observed, i.e., increasing correlation with MULTIFAN-CL recruitment and biomass estimates but decreasing spatial correlation between observed and predicted catch may be not too surprising. When increasing α, the recruitment becomes more dependent on regions with high P/F ratio, with an increasing amplitude of fluctuations and an overall distribution that is more patchy and contrasted. Consequently, if the movement of young and adult tuna is not perfectly described in the model, negative effects in the correlation due to small shifts in the spatial prediction will increase with the increasing patchiness (increasing α) of recruitment.

The large interannual variations in the recruitment (Fig. 11, 13) are related to the ENSO (El Niño Southern Oscillation) events, the recruitment being the highest during El Niño years (1972, 1982-83, 1987, 1990) and the lowest during La Niña years (1974-76, 1988-89). The simulations using $\alpha>0$ predict that the main skipjack spawning ground occurs in the western Pacific between Indonesia and Papua New Guinea, with a general decreasing gradient from west to east (Fig. 14). During El Niño events the recruitment of juvenile increases drastically with a spatial extension to the central Pacific, while during La Niña it is contracted in the western Pacific and with a lower level (Fig. 14 and 15). It is also worth noting that a seasonal pattern appears in Figure 15 in the far western Pacific.

A large proportion of these recruits moves either to Japan following the Kuroshio or to the central Pacific in the convergence zone between the warm pool and the cold tongue (Fig 15 and 16) as already described in previous studies (Lehodey et al. 1997, 1998, Lehodey 2001) and in agreement with the results of the skipjack MULTIFAN-CL analysis (Hampton et al 2001).

Finally, the relation of the recruitment to the stock of adults has been tested. Stock-recruitment relationships are usually justified by compensatory mechanisms. The most frequently suggested are changes in larvae survival rates in relation to the concentration of predators and the competition for food. As these mechanisms are already considered in the recruitment index with the P/F ratio, only the relation of proportionality remains. It was tested by introducing the log of the adult biomass in the calculation of the spawning habitat index for the simulation using $\alpha = 0.75$. The results show only slight changes in the predicted distributions and fluctuations of biomass (Fig. 17). This is because the distribution of adult biomass is very close to the distribution of the spawning habitat defined with temperature and P/F ratio. Maximum relative variations (but low in absolute value) occur in regions representing the extreme ranges of distribution of the species. However, this relation would likely have more influence on the recruitment of tuna species with longer life span and important spatial shifts between spawning and feeding grounds (e.g., albacore, bluefin).

Conclusion

The spatial prediction of tuna population dynamics in SEPODYM is strongly dependent on the quality of environmental data used. Despite some limitations, the use of a new set of predicted primary production and physical data has considerably extended the analysis, as the simulations cover all the Pacific Ocean since 1955, and also because prediction of primary production are improving. The next simulations should include the period between 1992 to the present, allowing comparisons with recent and numerous observed data (e.g., SeaWiFS) including the strong El Niño of 1997-98 followed by the long La Niña event of 1998-2001.

Though the spatial coverage includes the full range of the stock, there are still some limitations, particularly for the Japanese fishery in the sub-tropical region. Future improvements of the physical model should certainly improve the prediction for this fishery. The generally lower prediction in the eastern Pacific Ocean needs also to be analysed in details. A collaborative study with the IATTC would be very useful to compare recruitment and biomass with estimates from a statistical model (A-SCALA).

Recruitment mechanisms are fundamental processes in population dynamics. The spatial model SEPODYM is particularly well suited to test hypotheses on these mechanisms and on

the stock-recruitment relationships. The results concerning the skipjack recruitment are more than encouraging. However, with the improvement of recruitment prediction it is necessary to improve the parameterization of young and adult movements. In particular, advection and diffusion coefficients of tuna could be age-dependent to have a more realistic description of the physical capability of movement associated with the size of fish.

These results confirm the impact of the ENSO variability with a positive (negative) effect of El Niño (La Niña) events on the recruitment that is propagated into the stock in the following two years. Therefore, after the 1997-98 El Niño event and the associated high record of skipjack catch in 1998-2000, the last La Niña episode of 1998-2001 should lead to a decrease of the skipjack stock biomass in the next two years.

Reference List

Bertignac,M., Lehodey,P., and Hampton,J. 1998. A spatial population dynamics simulation model of tropical tunas using a habitat index based on environmental parameters. Fish.Oceanogr. **7**: 326-335.

Bills, P. J and Sibert, J. R. 1997. Design of Tag-Recapture experiments for estimating yellowfin tuna stock dynamics, mortality, and fishery interactions. Joint Institute for Marine and Atmospheric Research.

Chai,F., Dugdale,R.C., Peng,T.-H., and Barber,R.T. 2001. One Dimensional Ecosystem Model of the Equatorial Pacific Upwelling System, Part I: Model Development and Silicon and Nitrogen Cycle. Deep Sea Research II.

Hampton J., Ogura M., and Fournier D. 2001. Stock assessment of skipjack tuna in the western and central Pacific Ocean. 14th SCTB, SPC, Noumea, New Caledonia. 32 pp.

Iverson,R.L. 1990. Control of marine fish production. Limnol.Oceanogr. **35**: 1593-1604.

Lehodey, P. 2000. Update on the Spatial Environmental Population Dynamics Model: SEPODYM. Secretariat of the Pacific Community No. RG-2.

Lehodey,P. 2001. The pelagic ecosystem of the tropical Pacific Ocean: Dynamic spatial modelling and biological consequences of ENSO. Prog.Oceanogr., 30 pp.

Lehodey,P., Andre,J.-M., Bertignac,M., Hampton,J., Stoens,A., Menkes,C., Memery,L., and Grima,N. 1998. Predicting skipjack tuna forage distributions in the equatorial Pacific using a coupled dynamical bio-geochemical model. Fish.Oceanogr. **7**: 317-325.

Lehodey,P., Bertignac,M., Hampton,J., Lewis,A., and Picaut,J. 1997. El Nino Southern Oscillation and tuna in the western Pacific. Nature **389**: 715-718.

Li, X.; Chao, Y.; McWilliams, J.C.; Fu, L-L. 2001. A Comparison of Two Vertical-Mixing Schemes in a Pacific Ocean General Circulation Model. *Journal of Climate*, **14 (**7): 1377-1398

Press,W.H., Teukolsky,S.A., Vetterling,W.T., and Flannery,B.P. 1992. Numerical recipes in C. The art of scientific computing. Cambridge University Press, Cambridge.

Schaefer, K. M. 1998. Reproductive biology of yellowfin tuna (*Thunnus albacares*) in the eastern Pacific Ocean. Inter-American Tropical Tuna Commission No. 21.

Sibert,J.R., Hampton,J., Fournier,D.A., and Bills,P.J. 1999. An advection-diffusion-reaction model for the estimation of fish movement parameters from tagging data, with application to skipjack tuna (*Katsuwonus pelamis*). Can.J.Fish.Aqu.Sci. **56**: 925-938.

Sibert,J.R. and Fournier,D.A. 1994. Evaluation of advection-diffusion equations for estimation of movement patterns from tag recapture data. *In* Interactions of Pacific tuna fisheries. *Edited by* R.S.Shomura, J.Majkowski, and S.Langi. FAO, Rome pp. 108-121.

Stoens,A., Menkes,C., Radenac,M.-H., Dandonneau,Y., Grima,N., Eldin,G., Memery,L., Navarette,C., Andre,J.-M., Moutin,T., and Raimbault,P. 1999. The coupled physical-new production system in the equatorial Pacific during the 1992-95 El Niño. J.Geophys.Res. **104**: 3323-3339.

Table 1. Annual fishin effort (f in days) and catch (c in metric tonnes) for the ten fleets described in the SEPODYM simulations: EPPS, Eastern Pacific purse seine; JPPS, Japan purse seine; KRPS, Korean purse seine; TWPS, Taiwan purse seine; USPS, U.S.A. purse seine; SBPS, Solomon purse seine; JPPL, Japan pole and line; SBPL, Solomon pole and line; FJPL, Fiji pole and line; PHIN, Philippine-Indonesia domestic.

	EPPS		JPPS		KRPS		TWPS		USPS		SBPS		JPPL		SBPL		FJPL		PHIN	
	f	c	f	c	F	c	f	c	f	c	f	c	f	c	f	c	f	c	f	c
1972			145	192									34276	77234					1171	4668
1973			248	1954									52321	167323					3845	5004
1974			303	2117									33276	171597					1496	5748
1975			422	4247									37185	77616					1304	624
1976			790	7677									53136	93554			273	566	1988	4968
1977			627	10715									33605	118690			548	1282	2056	13548
1978			1211	19978									40943	229098			752	1389	1848	8172
1979			1236	22908									41595	125198			427	3141	2034	17928
1981	21828	67763	2131	29489	220	1139			1849	15092			40881	192069	4629	14190	2174	4819	4335	26628
1982	20646	73821	3083	59167	462	6289			4245	48110			56611	154696	4473	10368	1367	3300	5559	40396
1983	15608	30106	6172	57814	316	9450	529	7811	7318	109868			31950	184365	5357	21153	937	2156	7397	52713
1984	15886	31415	6084	64158	643	9025	1189	13847	5577	106514	296	2177	46769	172998	5666	23460	923	3225	5915	11574
1985	13901	25023	6625	68467	445	6738	1761	18376	4551	50429	200	1911	34241	107187	6580	20861	1122	3032	6335	5352
1986	16120	40449	5799	102103	592	12554	4057	28321	5522	60965	149	3262	26553	159535	6079	21981	984	1966	6039	5529
1987	18284	42775	5488	76481	1611	31414	7715	40710	5770	74189	215	3341	28942	140989	5193	18624	838	2235	7755	43472
1988	20055	51730	6621	85406	1438	54828	9210	45172	9143	138523	324	4856	22721	144242	7393	27494	859	3489	6241	53628
1989	14799	49513	5354	74213	1980	60118	6931	65289	5388	85703	264	3709	22555	112892	5116	20420	1048	3413	8776	61836
1991	19493	41586	5938	62773	4876	119621	26147	88136	7253	97235	228	4059	14495	124268	5939	30000	1603	3360	11820	84258
1992	19544	47478	5071	83723	4772	59123	16543	87098	5133	125239	375	5444	21782	103088	4035	12102	1609	3486	5659	792

Table 2. Comparisons of statistical correlations between predicted and observed catch and with Multifan-Cl estimates of recruitment and adult biomass, for the simulations with 4 different values of α in the calculation of the spawning habitat index. EPO: purse seine catch in the eastern Pacific Ocean. WCPO: purse seine catch in the western central Pacific Ocean. JPPL: pole and line catch of the Japanese fleet. Due to the bias in the temperature fields at high latitude, the summer catch (July to September) of the Japanese pole and line fleet (JPPL) is not included in the spatial correlation.

	Simulation	*α = 0*	*α = 0.5*	*α = 0.75*	*α = 1*
Total monthly catch by fleet					
Correlation between predicted and observed	1 – epps	0.514	0.470	0.448	0.424
	2 – jpps	0.810	0.796	0.796	0.781
	3 – krps	0.851	0.848	0.860	0.869
	4 – twps	0.814	0.834	0.815	0.777
	5 – usps	0.761	0.791	0.788	0.764
	6 – sbps	0.575	0.611	0.614	0.614
	7 – jppl	0.221	0.189	0.201	0.199
	8 – sbpl	0.734	0.719	0.702	0.684
	9 – fjpl	0.772	0.769	0.778	0.782
	10 – phin	0.865	0.859	0.849	0.833
	Average	**0.690**	**0.690**	**0.685**	**0.673**
Spatial monthly catch (degree square)					
Correlation between predicted and observed catch	EPO	0.387	0.352	0.330	0.315
	WCPO	0.683	0.688	0.687	0.666
	JPPL	0.735	0.713	0.705	0.686
	Average	**0.602**	**0.584**	**0.574**	**0.555**
Comparison with MultifanCL					
Recruitment Correlation between predicted R by sepodym and MultifanCL	area 1	-0.113	0.077	0.203	0.304
	area 2	0.280	0.150	0.234	0.346
	area 3	-0.052	-0.169	-0.083	0.124
	area 4	-0.300	-0.065	0.006	0.072
	area 5	-0.463	0.305	0.407	0.459
	area 6	0.390	0.326	0.318	0.323
	all areas	**0.136**	**0.451**	**0.528**	**0.576**
Adult Biomass Correlation between predicted adult biomass by sepodym and MultifanCL	area 1	-0.210	-0.318	-0.316	-0.296
	area 2	-0.157	0.074	0.178	0.249
	area 3	0.251	0.359	0.392	0.404
	area 4	-0.246	-0.040	-0.010	0.006
	area 5	-0.498	-0.212	-0.074	0.048
	area 6	-0.143	0.228	0.375	0.503
	all areas	**-0.458**	**-0.036**	**0.152**	**0.305**

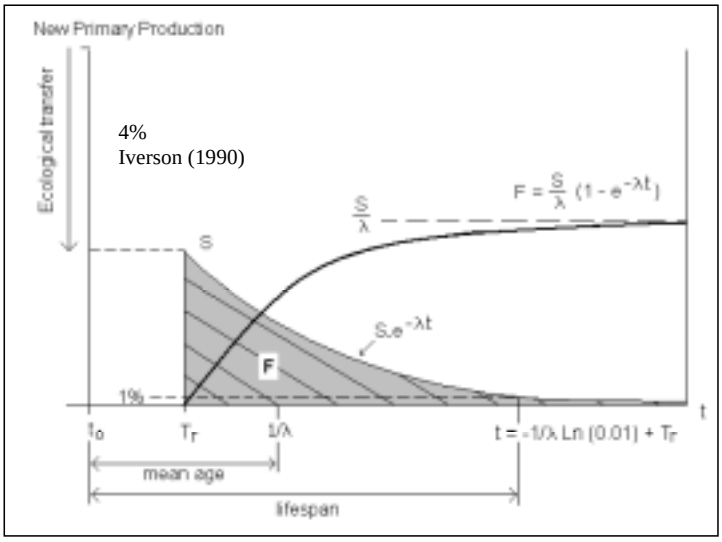

Figure 1. Transfer with time of primary production towards forage according to the model (*S* is assumed constant). The thin curve describes the evolution in time of a single source of primary production. The thick curve gives the total forage population (from Lehodey 2001).

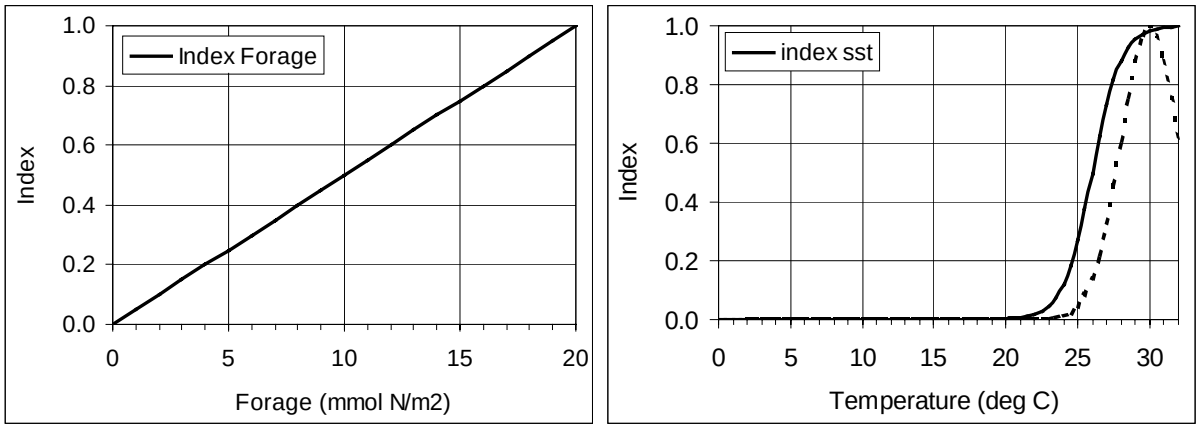

Figure 2. Functions used in the definition of the skipjack habitat. The habitat index is the product of the two functions. The dotted curve describes the function used in previous simulations (Lehodey 2001).

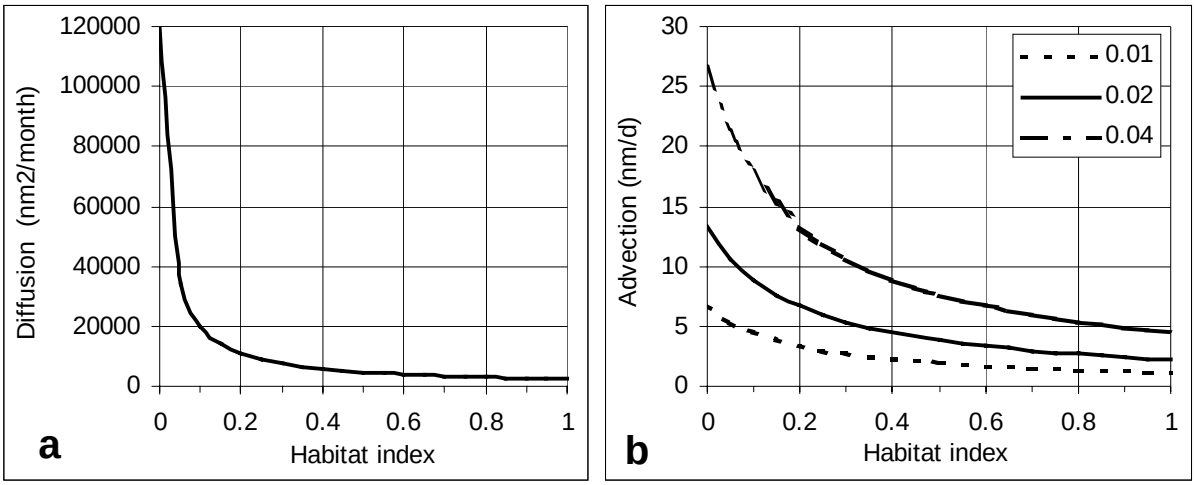

Figure 3. Functions used to describe change in tuna movement according to the habitat index values. a, diffusion and b, advection for three different values of habitat gradient. Typically, 80% of habitat gradient values are below 0.01 and more than 90% below 0.04.

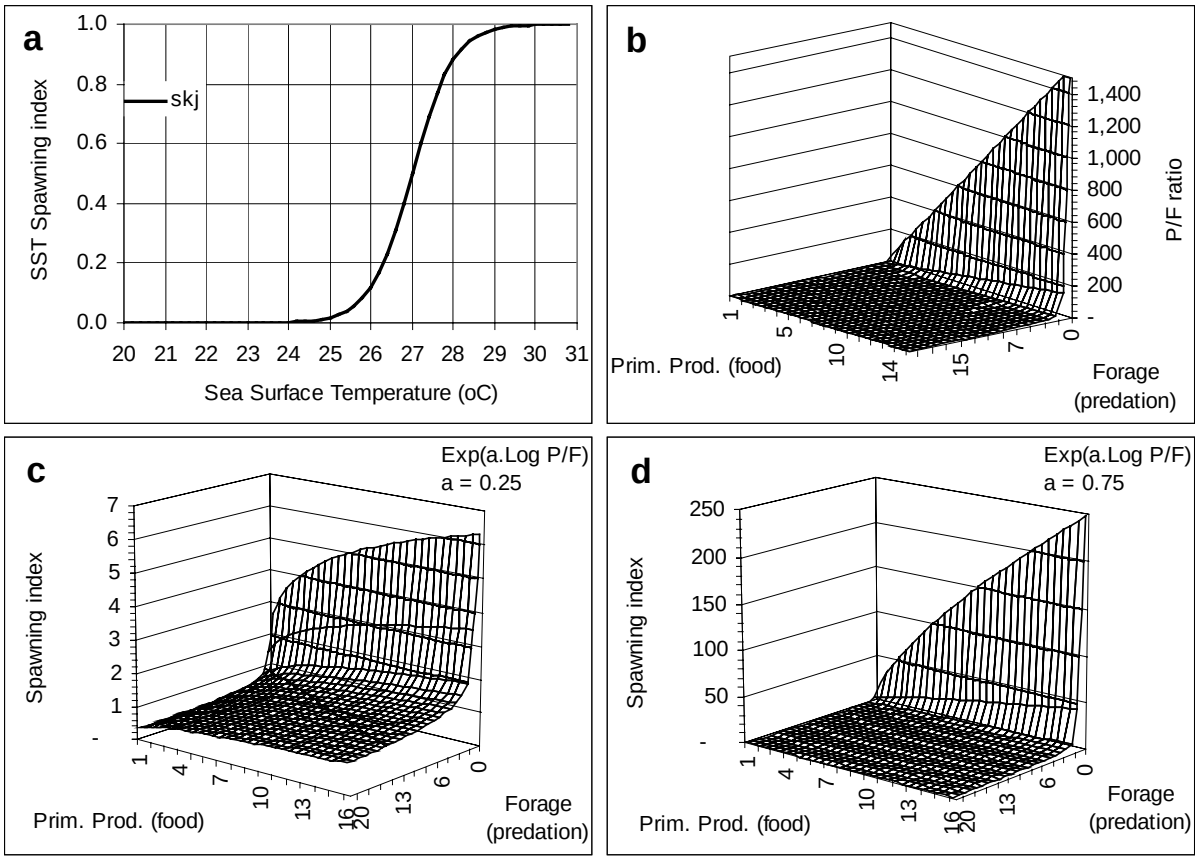

Figure 4. Spawning habitat index. Temperature function used for skipjack spawning habitat index (a), P/F ratio (b) and illustration of change in spawning index (c and d) related to P/F ratio for two values of α.

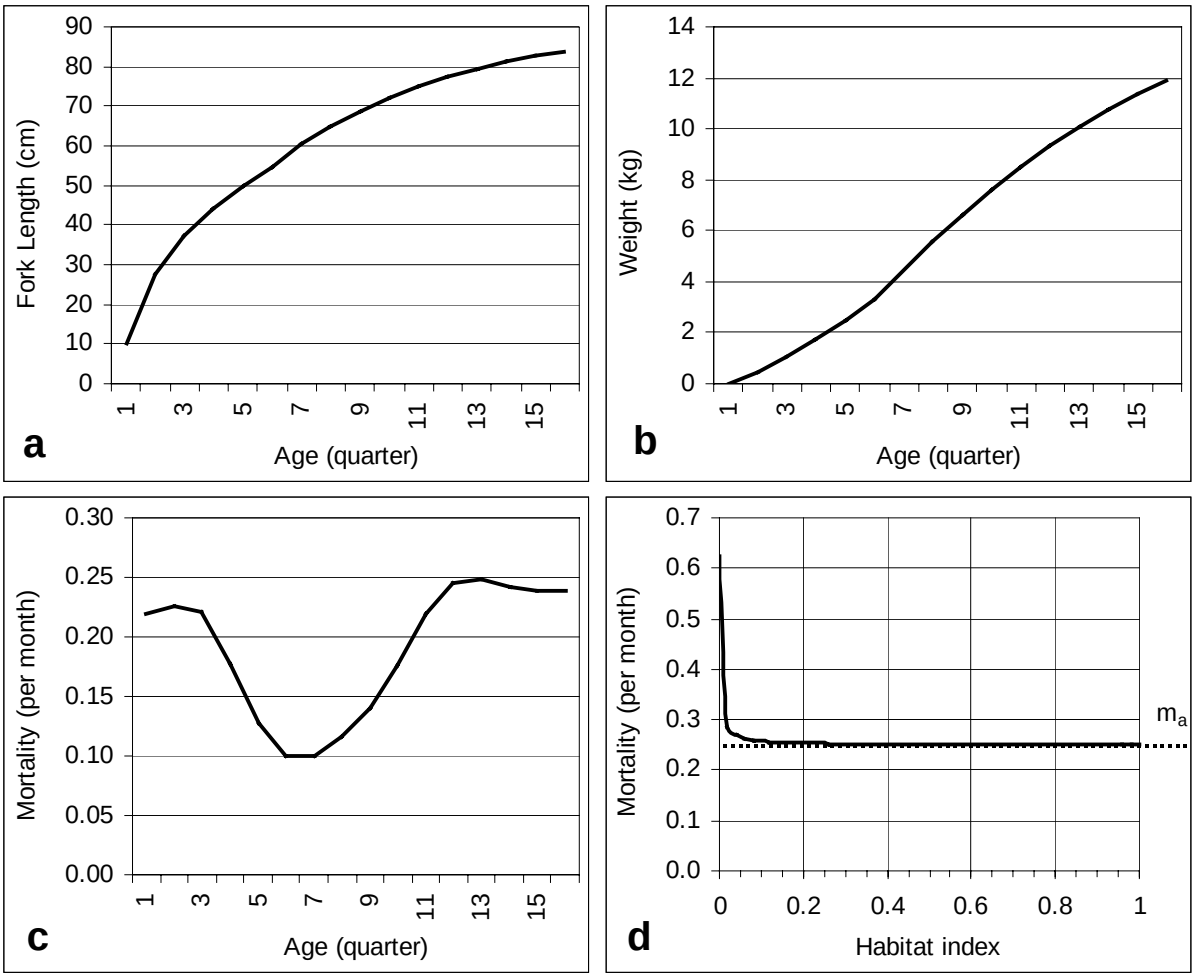

Figure 5. Skipjack mean length at age (a), mean weight at age (b) and mean natural mortality at age (c) according to the MULTIFAN-CL estimates (Hampton et al. 2001). At very low values of habitat index, a function (d) is used to increase the natural mortality (m_a is the natural mortality at age a).

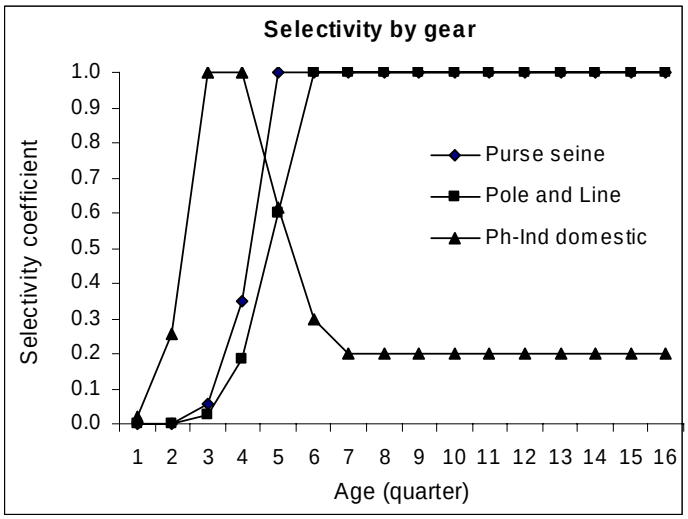

Figure 6 . Selectivity by gear used in the SEPODYM skipjack application.

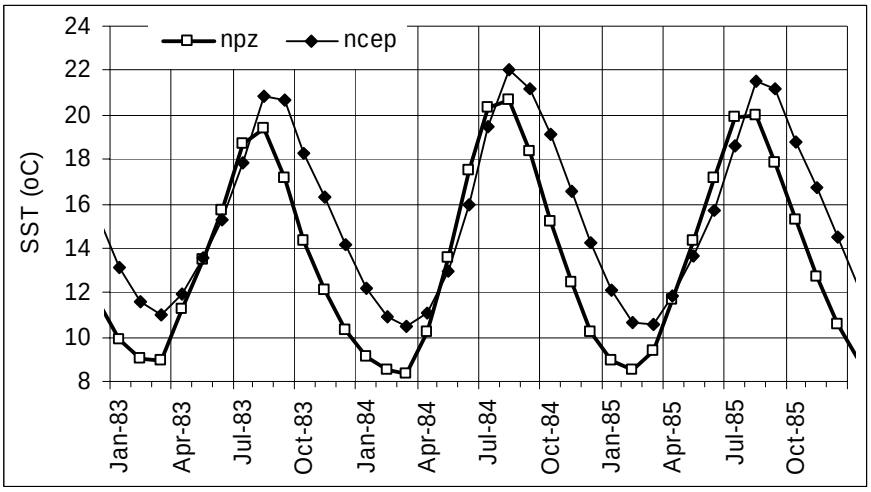

Figure 7. Comparison between averaged sea surface temperature in the area 35N-40N, 140E-180E between the physical model used for the npz and sepodym simulation and the model used by the National Climate and Environmental Programme (NCEP, USA).

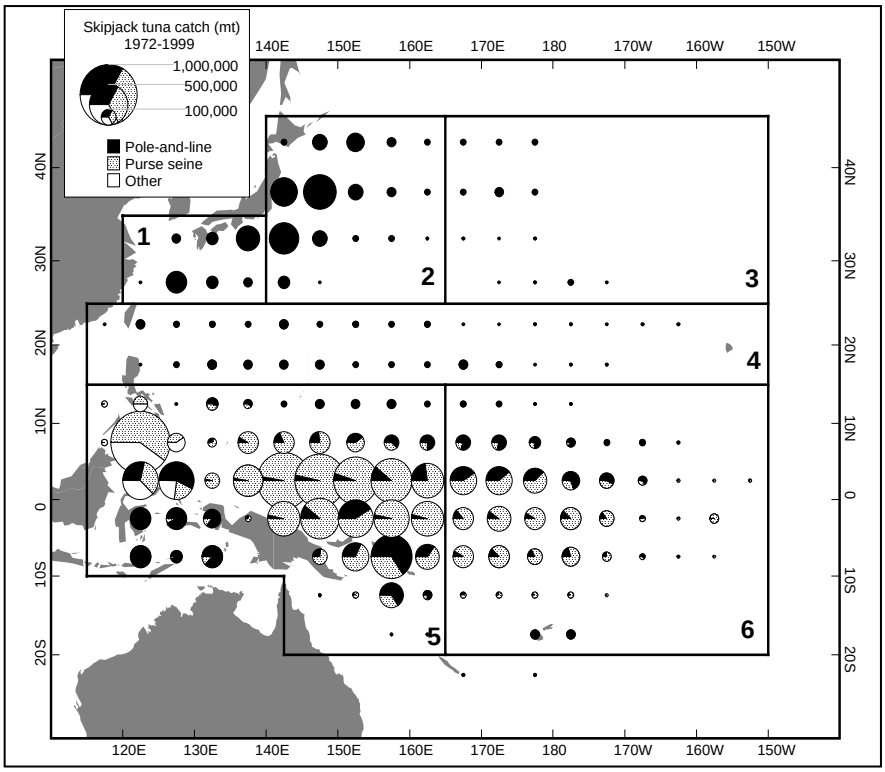

Figure 8. Geographical areas defined for the skipjack Multifan-CL application.

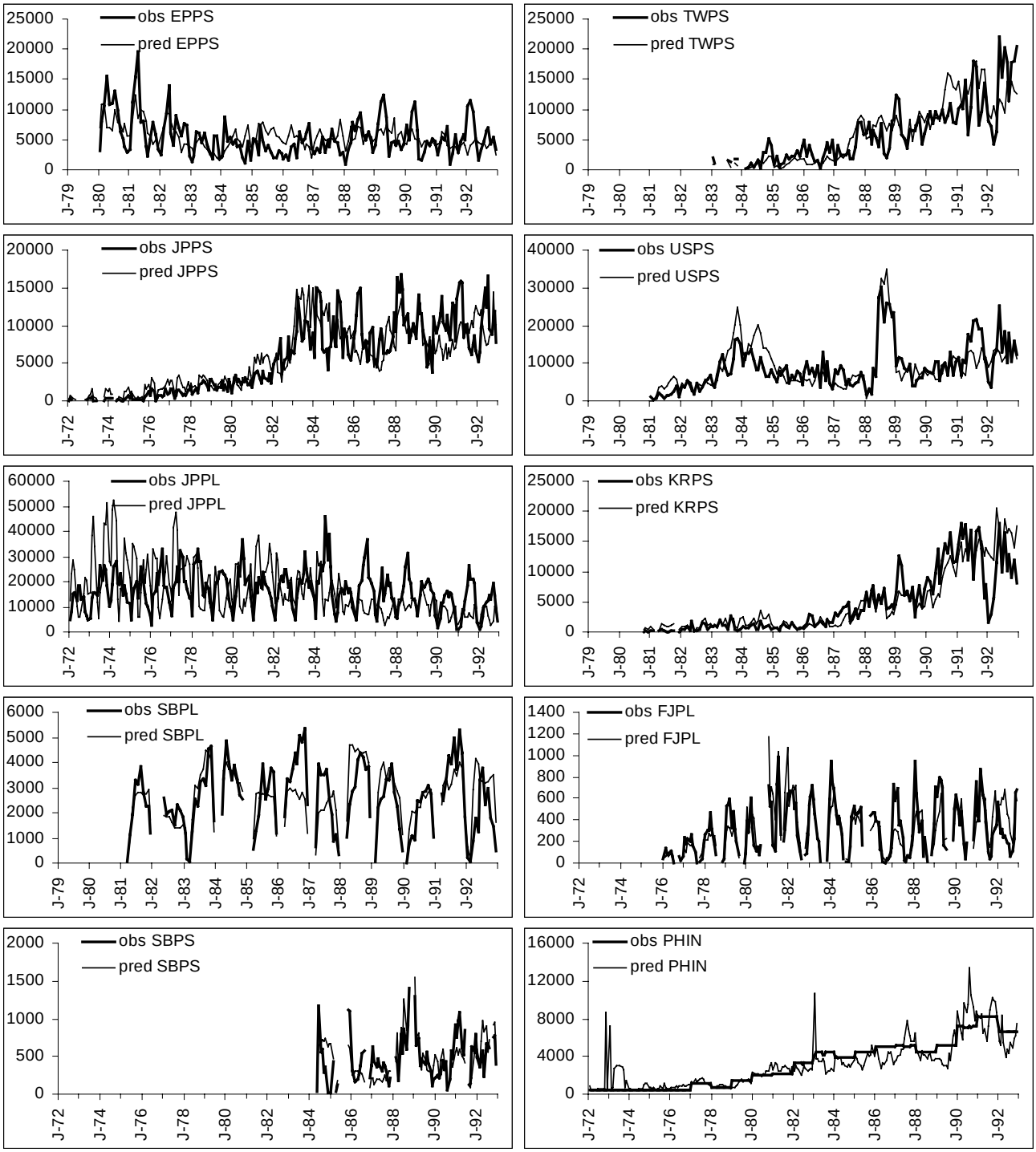

Figure 9. Total observed (thick curve) and predicted (thin curve) skipjack monthly catch by fleet (metric tonnes) for the simulation with $\alpha = 0.75$.

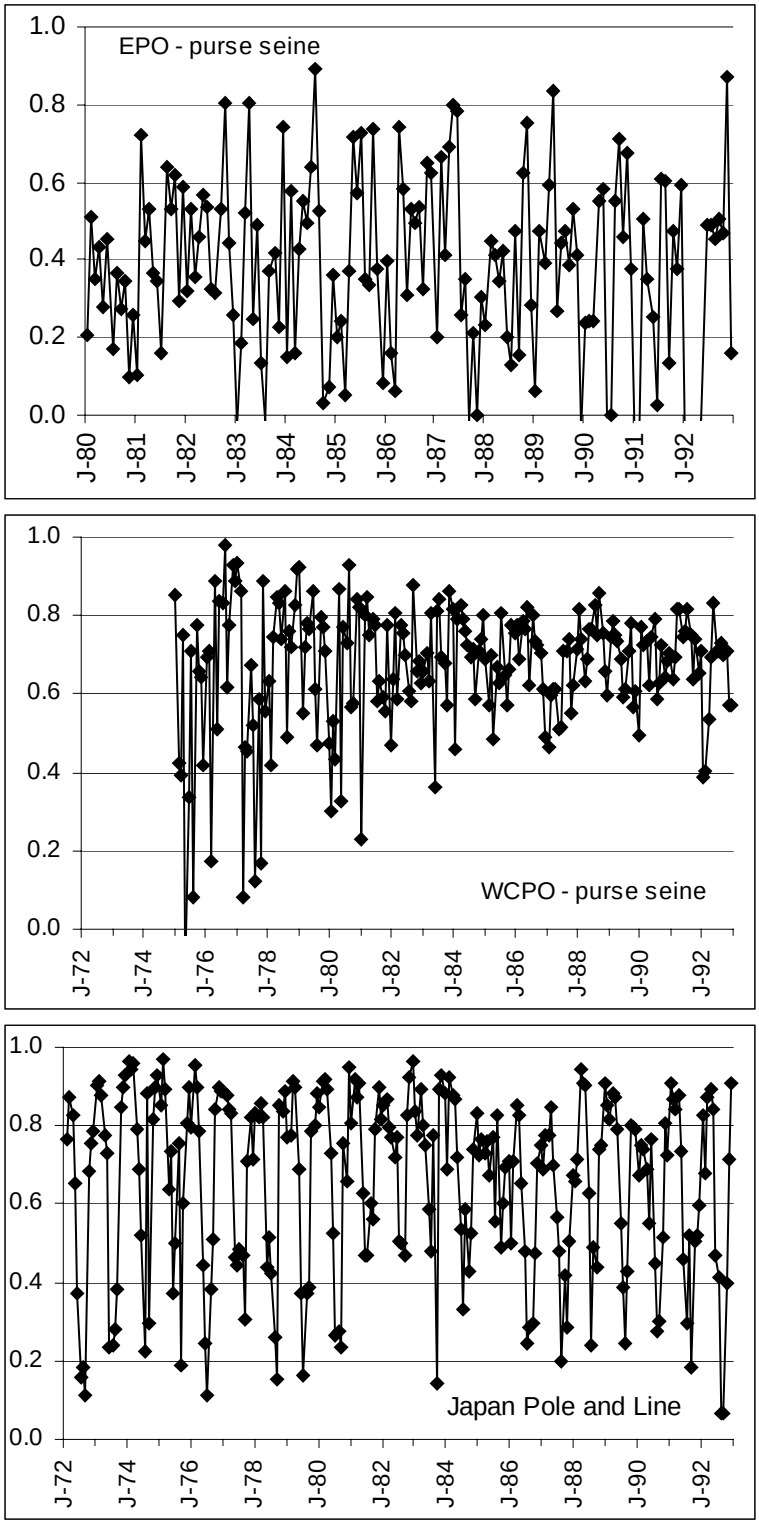

Figure 10. Monthly spatial (one degree square resolution) correlation between observed and predicted skipjack catch for the purse seiners in the eastern Pacific (EPO), western central Pacific (WCPO) and the Japan pole and line fleet (simulation with $\alpha = 0.5$).

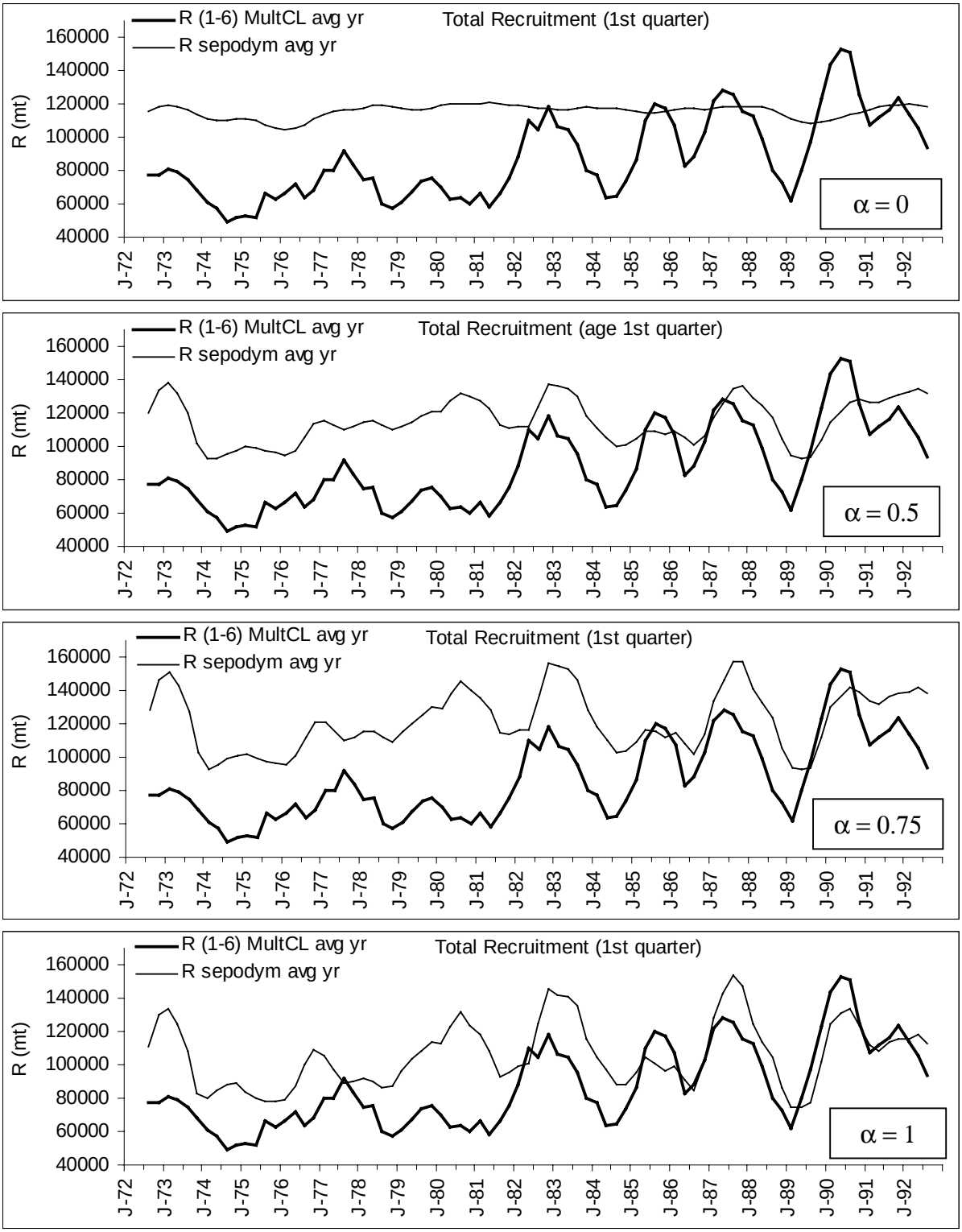

Figure 11. Comparison of recruitment estimates from MULTIFAN-CL and SEPODYM (total biomass of fish of age 1 quarter in the areas 1 to 6) for increasing values of α.

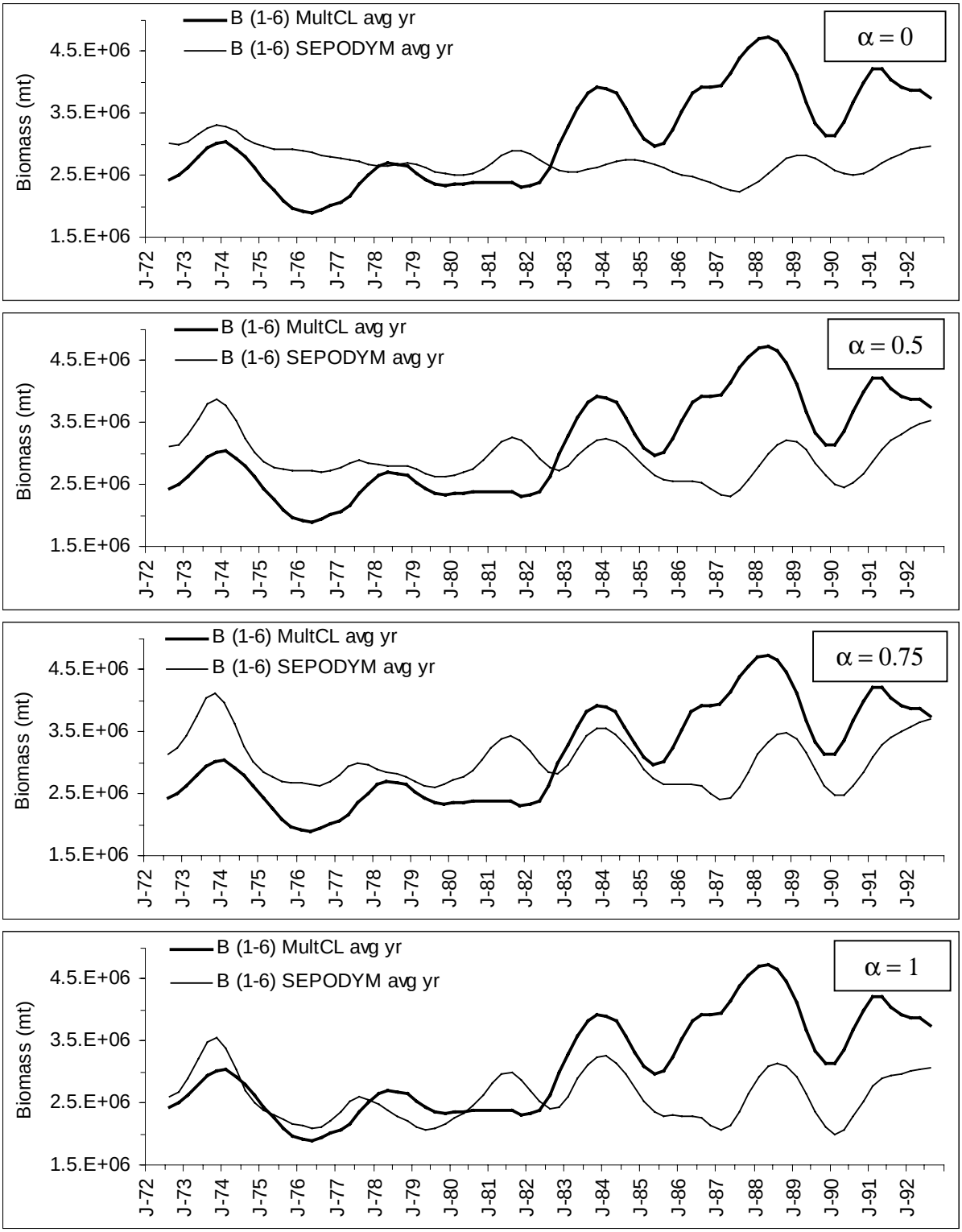

Figure 12. Comparison of adult skipjack biomass estimates from MULTIFAN-CL and SEPODYM for increasing values of α (total biomass of fish of age 4 to 16 quarter in the areas 1 to 6).

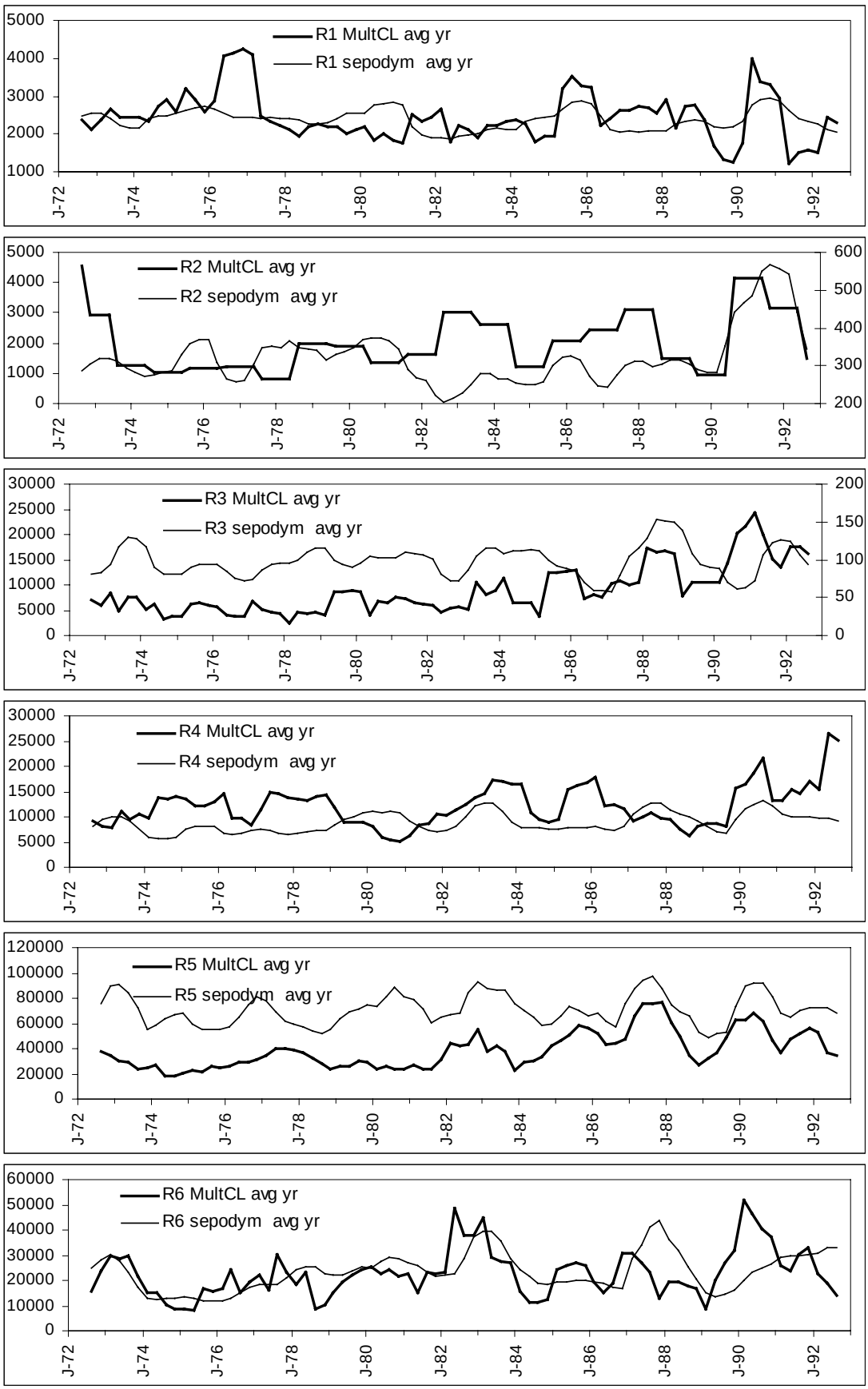

Figure 13. Comparison of recruitment estimates (total biomass of fish of age 1 quarter) from MULTIFAN-CL and SEPODYM ($\alpha = 1$) in the 6 areas used in the MULTIFAN-CL application.

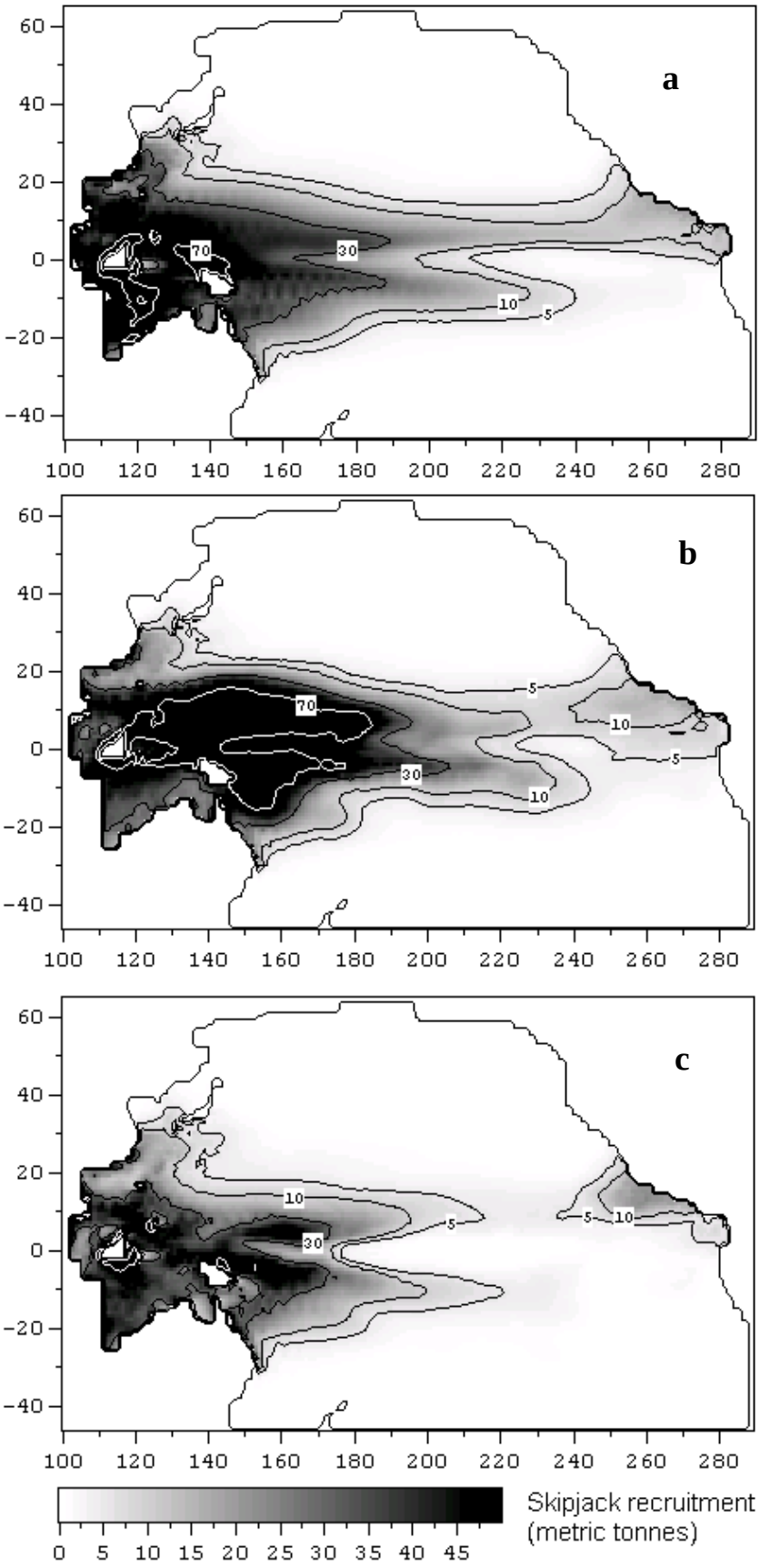

Figure 14. Skipjack recruitment ($\alpha = 0.75$). (a) average over 1972-1992, (b) El Niño (Oct 1982-Mar 1983), (c) La Niña (Oct 1988-Mar 1989)

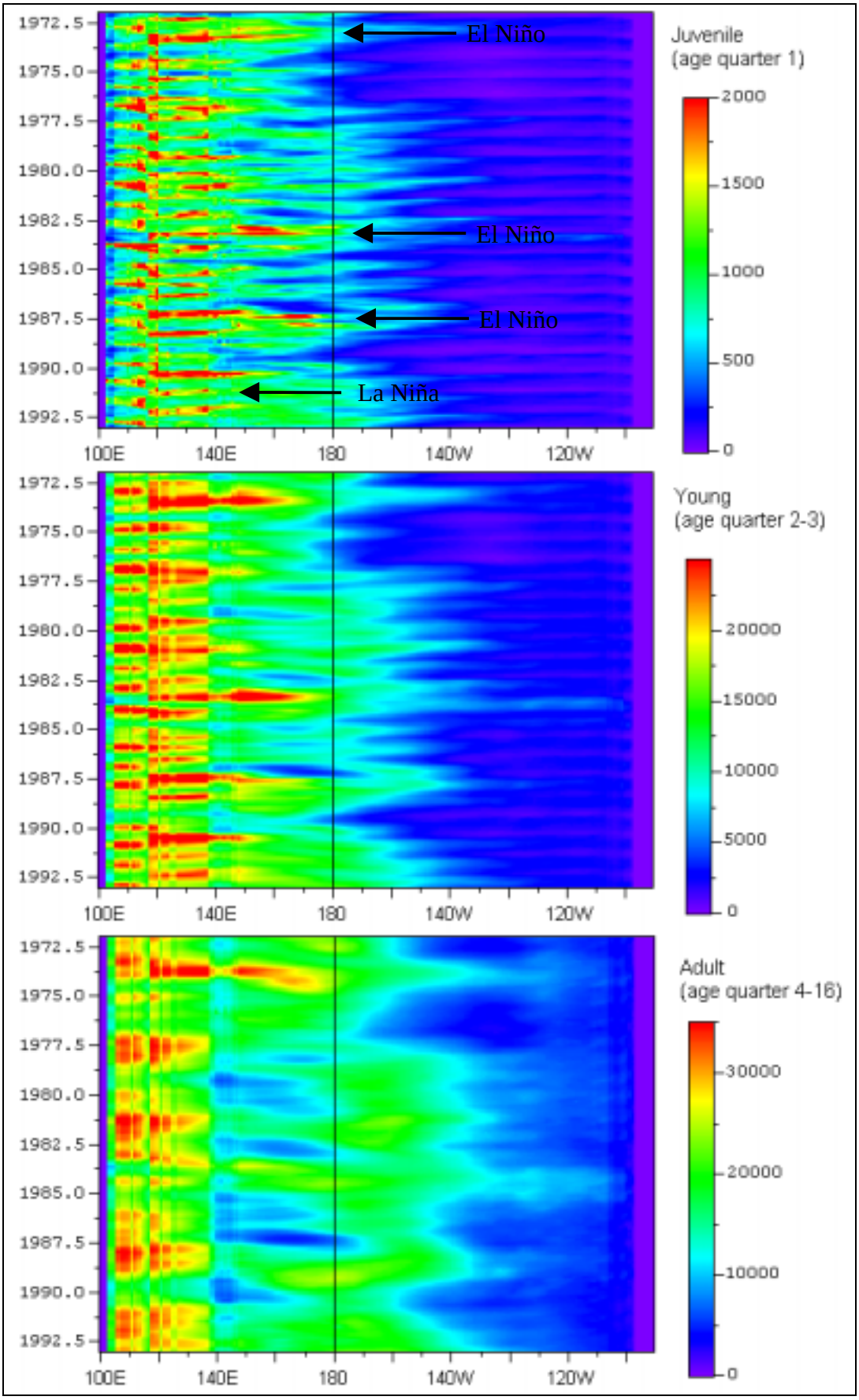

Figure 15. Time longitude plot of the predicted (α = 0.75) total biomass of juvenile, young and adult skipjack in the equatorial band 10^{o}N-10^{o}S.

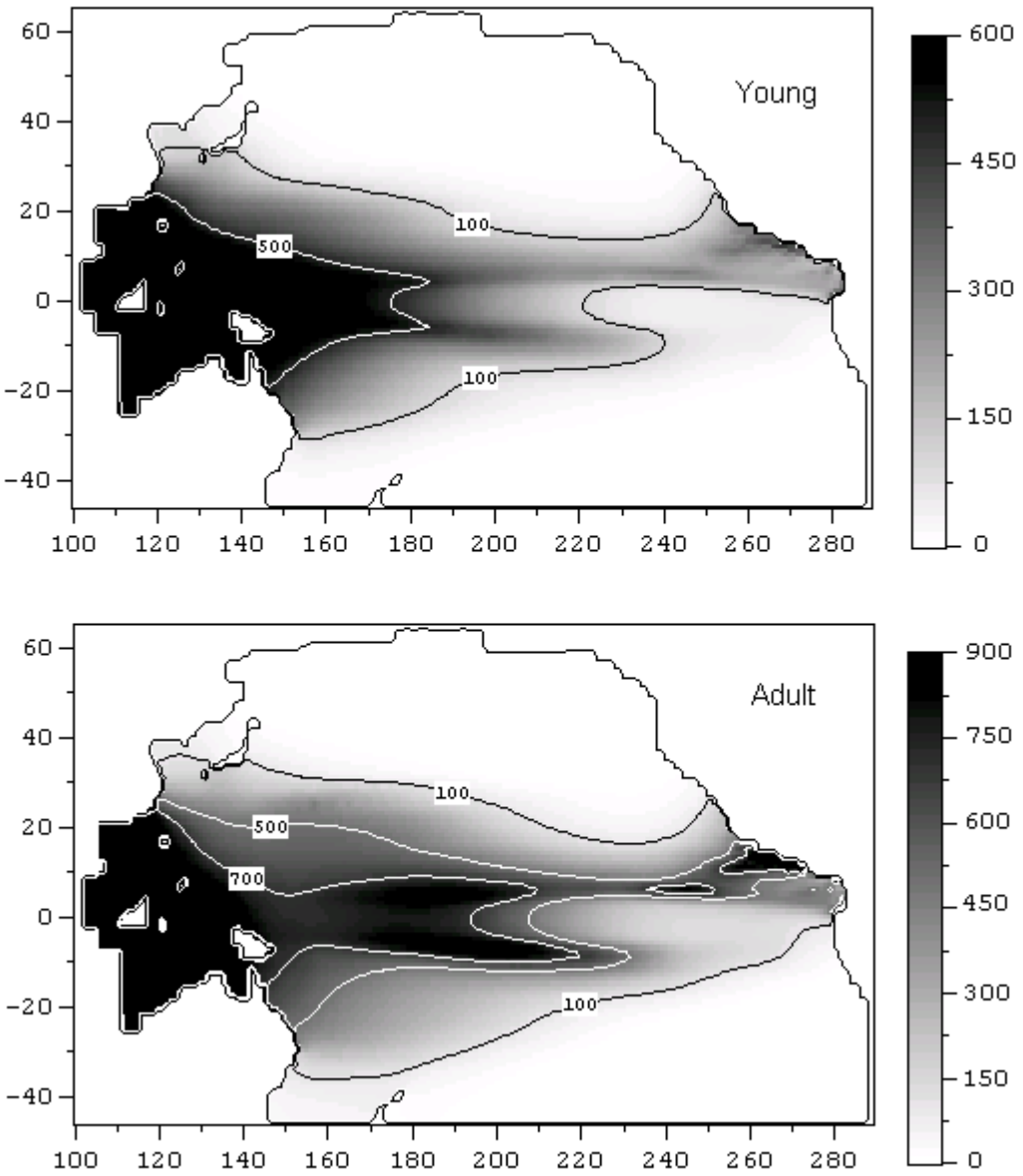

Figure 16. Average predicted (α = 0.75) spatial distribution over 1972-1992 of the biomass (metric tonnes per degree square) of young (age 2 and 3 quarter) and adult (age 4 to 16 quarter) skipjack

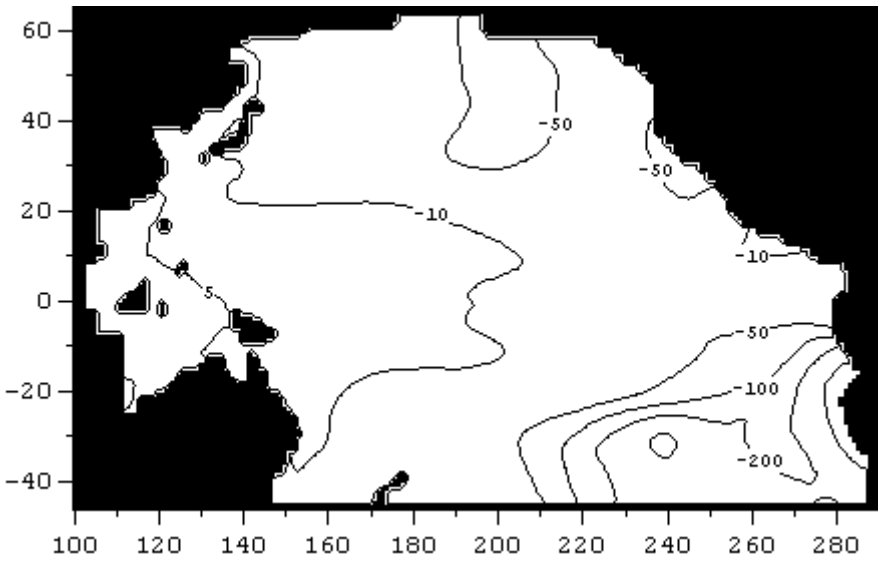

Figure 17. Change in the recruitment (% of biomass) for the simulation with α = 0.75 when the spawning index is made proportional to the log of the adult biomass.